

Chromium and Vanadium Carbide and Nitride Coatings obtained by TRD techniques on UNI 42CrMoS4 (AISI 4140) steel

Mattia Biesuz[#] University of Trento, Department of Industrial Engineering
Via Sommarive, 9 - 38123 Trento- Italy
mattia.biesuz@unitn.it

Vincenzo M. Sglavo University of Trento, Department of Industrial Engineering
Via Sommarive, 9 - 38123 Trento- Italy
vincenzo.sglavo@unitn.it

Abstract

Different Thermo-Reactive Diffusion and Deposition (TRD) treatments have been analysed in the present work. The processes were carried out on UNI 42CrMoS4 (AISI 4140) steel both in the nitrided and bare state at temperatures of 825, 900 and 1000°C, the samples being quenched in water afterwards. Hard, compact and adherent vanadium and chromium carbide and vanadium nitride coatings, mainly consisting of Cr_7C_3 , V_6C_5 and VN, were obtained using different processing conditions. Biphasic layers composed by two different carbides were also obtained. The average micro-hardness of the coatings ranged from 1717 ± 170 to $2451 \pm 236 \text{ HV}_{0.02}$ whereas R_a values between 0.2 and $1.2 \mu\text{m}$ were measured. The kinetics of the coatings growth was also studied on the basis of SEM observations. It was demonstrated that the layer thickness is related to the time by a parabolic law and to the temperature by an Arrhenius-like behaviour.

Keywords: coatings, carbide, nitride, TRD, diffusion

Published version available at
<https://www.sciencedirect.com/science/article/pii/S025789721530493X>

[#] Corresponding author

1 Introduction

The production of hard carbide and nitride coatings on steel represents an important research and technological field for engineering applications where high wear, oxidation and corrosion resistance and, consequently, extended component lifetime are required.

Nowadays, carbide and nitride coatings are widely used in tribological applications such as tools, moulds, mechanical parts and dies for metals, plastics and glass working. Two different deposition technologies are conventionally used, chemical vapour deposition (CVD) and physical vapour deposition (PVD), which, nevertheless present some drawbacks such as the plant investment cost and the need of a vacuum or highly controlled atmosphere [1].

Thermo-Reactive Diffusion and Deposition (TRD) process offers an interesting alternative for the production of hard coatings. As a matter of fact, TRD is much simpler, environmental friendly [2] and less expensive if compared with other coating processes. TRD treatments allow the production of high quality ceramic coatings with important properties in terms of hardness, adhesion, toughness and heat resistance [3-6]. Nevertheless, also this technology has some drawbacks since (i) only carbon- (or nitrogen-) containing substrates can be treated and (ii) the temperature process is typically higher than the austenization temperature of steel, thus leading to possible distortions of the component [3].

The most common TRD process uses a molten salts bath (typically borax). At first, the borax is melted and then the carbide forming elements (CFE) powders are added and dissolved in the bath. Also a reducing agent such as aluminium is typically added to avoid the CFE oxidation [2,3,7-10]. Nevertheless, different TRD techniques are available using molten chloride [10-13] or gas phases (pack method [4-6,14-16] or fluidized bed [10,17,18]).

The reaction between the CFE from the bath and the carbon (and/or nitrogen), which diffuses from the substrate, causes the carbide (and/or nitride) formation on the steel surface. All metals with limited free energy for carbide (nitride) formation and forming oxides less stable than B_2O_3 can be used as CFE [7]. Among them, chromium and vanadium represent a good

choice because of their high affinity with carbon and nitrogen and because of their carbide and nitride excellent properties in terms of wear, oxidation and chemical resistance.

In spite of the potential advantages pointed out above, TRD technology has not been extensively used and, correspondingly, the scientific literature is relatively limited if compared with other deposition technologies (like, for example, CVD or PVD). In particular, very few data can be found in the literature on the treatments in baths containing more than one CFE. Moreover, the surface characterization of the coatings produced by TRD is often very limited (especially in term of roughness measurement) and this prevents a reliable comprehension of the applicability of the TRD process.

In order to understand better possible applications, benefits and limitations of TRD technology on steel components, in the present work we produced chromium and vanadium carbide and nitride layers on UNI 42CrMoS4 steel by using the molten salts TRD method; this allows to analyse the effects of mixing different CFE powders in the same bath, identify the influence of the main process parameters (time, temperature, bath) and study the coating growth kinetics.

2 Materials and Methods

2.1 Materials and Process

TRD process was carried out on a medium carbon steel, UNI 42CrMoS4, provided in form of discs with diameter of 20 mm and thickness of 5 mm; both quenched and tempered (Q/T) samples and nitrided (N) disks were considered. The nominal and actual steel composition is reported in Table I.

The surface of the nitrided samples is characterized by a compound layer (about 10 μm) mainly composed of $\text{Fe}_4\text{N}/\text{Fe}_3\text{N}$, the nitrogen diffusion zone extending for about 200 μm underneath; the surface hardness is $670 \pm 10 \text{ HV}_{0.1}$.

The surface of the samples was polished to obtain a roughness $R_a = 0.1\text{-}0.5\text{ }\mu\text{m}$. Before the TRD process, the samples were cleaned and degreased with acetone for 5 min in an ultrasonic bath.

The specimens were treated within sillimanite crucibles placed within an electrical furnace working in static air. Five different baths were tested, each one containing 85 wt% borax, 12 wt% CFE (chromium or ferrovanadium or a mixture of both) and 3 wt% aluminium used as reducing agent. Chromium powder grain size was smaller than $300\text{ }\mu\text{m}$ whereas for ferrovanadium (containing 79.5 wt% vanadium and 18.0 wt% iron) it was smaller than $150\text{ }\mu\text{m}$. The detailed composition of the used baths is summarized in Table II. At first, borax was melted in the crucible; then, the metallic powders were added and allowed to dissolve for 8 h at 1000°C .

Different duration and temperatures were tested, in the ranges 2-16 h and $825\text{-}1000^\circ\text{C}$, respectively. The different combinations of time, temperature, substrate and bath considered in the present work are summarized in Table III.

After the TRD treatment, the specimens were extracted from the molten bath and quenched in water; the samples were then cleaned in hot water before successive characterization.

2.2 Characterization

The samples were analyzed by optical microscope after being cut, polished using 4000 grid SiC paper and $3\text{ }\mu\text{m}$ diamond paste, degreased and etched with Nital (3 vol% nitric acid in ethanol). The samples were then observed by SEM (Jeol, JSM-5500) in order to study the cross-section morphology and the structure of the coating.

The composition of the ceramic layers was analysed by EDS microprobe (EDS2000, IXRF System) within SEM and mineralogical examination was carried out by XRD (Rigaku, D-Max diffractometer) with 2θ varying from 30° to 120° and using Cu $K\alpha$ radiation. The XRD analysis was performed on the surface of the coated specimens.

Vickers hardness was determined as average of ten measurements on the cross-section of the carbide/nitride layer using a maximum load of 0.2 N. The indentations were produced in the central part of each coating obtained at 1000°C with 4 h treatments. The distance from the border of the coating was 3-4 μm . The surface roughness was determined by a contact profilometer (Wave, Hommelwerke); for each sample two measurements were taken on orthogonal directions on a length of 5 mm with a speed of 0.1 mm/s.

3 Results and Discussion

For each combination of time, temperature, bath and substrate a carbide/nitride layer was produced on the steel, whose bulk structure is martensitic because of the final fast cooling process; the only exception is the nitrided steel treated in Cr12 bath where no coating is obtained at any time/temperature condition.

Figure 1 shows a Q/T sample treated with chromium (Cr12 bath) at 900°C for 16 h. The surface layer is substantially perfect in terms of adhesion and consistence; moreover, no cracks are present despite the cooling stresses and the phase transformations. The coating-substrate interface is extremely clean and smooth and the layer thickness is homogeneous. Similar results were obtained on specimens treated with ferrovanadium (Figure 2(b)), although some limited pores are present (especially in the external part of the coating). In some cases, when a nitrided substrate is used (Figure 2(a)), a non-perfectly flat interface between steel and coating is observed: this may be related to inhomogeneity of the original compound layer thickness after nitriding.

EDS analyses revealed that the coatings, produced in Cr12 and FeV12 baths, mainly contain chromium and vanadium respectively. As shown by the EDS linescan profiles, an effective chromium and iron interdiffusion can be pointed out in specimens treated in Cr12 bath (Figure 3(a)). As a matter of fact, the iron content decreases slowly moving from the core to the surface of the specimen and a wide area where both Fe and Cr are present can be observed.

Conversely, vanadium and iron do not mix significantly and the linescan shows very sharp concentration profiles (Fig. 3(b)). The observation confirms what Fan et al. [2] have already remarked and the effect can be probably due to the low solubility product of vanadium and carbon in austenite at TRD temperature. Conversely, chromium can be better solubilised [19], especially during the first stage of TRD process (before the ceramic coating formation). Then, during cooling, chromium precipitate in form of carbide as result of a decrease in the solubility product.

The baths containing both chromium and ferrovanadium (Cr_8FeV_4 , Cr_6FeV_6 , Cr_4FeV_8) allowed the production of biphasic coatings. Figures 4-5 show the presence of darker areas rich in vanadium and carbon, while the lighter ones contain chromium and carbon and small amounts of iron and vanadium. The extension of each phase becomes coarser moving from the inner to the external part of the coating (Fig. 5); this suggests that the grain size, as pointed out by Fan et al. [2], increases from the interface to the coating surface.

The two phases distribution was shown to be always homogeneous throughout the thickness. Therefore, there is not a significant time effect in determining the layer composition and the treating temperature does not have an important effect. Conversely, the content of the vanadium-rich phase (darker region) increases with the FeV powder load in the bath (Fig. 4).

The mineralogical composition of the coatings was determined by XRD analysis (Fig. 6). The nitrided steel (N) produced VN phase for treatments in FeV12 bath. The presence of V_6C_5 and Cr_7C_3 or $(\text{Cr},\text{Fe})_7\text{C}_3$ was instead detected on hardened (Q/T) steel treated in FeV12 and Cr12 bath, respectively. It is important to point out that the most stable phases VC and Cr_3C_2 do not form because of the carbon deficiency with respect to the amount of CFE provided by the bath, this suggesting that the reaction is controlled by the carbon diffusion (a more extensive discussion is reported below in the analysis of the process activation energy).

Biphasic layers appear to be composed by the same carbide previously indicated although the

peaks are slightly shifted. This can be probably related to thermal stresses induced by the presence of different phases and by solid solutions of different metals.

The XRD patterns obtained on the biphasic layers were analysed by Maud software and the resulting compositions are reported in Figure 7. One can observe that the carbides formation does not follow the rule of mixture: i.e., there is not a proportional relationship between the amount of the specific CFE (Cr or V) in the bath and the volumetric concentration of the corresponding carbide. In other words the expected Cr_7C_3 load is always lower than the measured one. It is assumed that the different growing rate of V_6C_5 and Cr_7C_3 can not account for by the observed behaviour.

One possible explanation can be related to the beneficial role of vanadium in the Cr_7C_3 growth, vanadium being always present (as for the EDS analyses) in the chromium carbide phase generated within the mixed baths. Therefore, it is thought that a portion of vanadium enters the Cr_7C_3 phase increasing its growing rate, the remaining forming the V_6C_5 phase. Other effects like different nucleation rates among the carbides or inhomogeneity in the salt bath can not be *a priori* excluded, anyway. Moreover, one has to point out that the V_6C_5 deficiency cannot be accounted for by thermodynamic effects as it has been suggested for the binary Nb-Cr TRD system [28]. As a matter of fact, at the TRD process temperature, the formation energy of vanadium ($-104 \div -106$ kJ/mol, for mole of carbon) is much lower than that of chromium ($-63 \div -67$, kJ/mol, for mole of carbon) [26] and this would lead to the formation of V_6C_5 rather than Cr_7C_3 .

The coatings thickness was measured by SEM as shown in Figures 8 and 9. At least five thickness measurements were collected for each condition. It is clear that the obtained results are influenced by the main process parameter, especially time (Fig. 8), temperature (Fig. 9), substrate and bath.

The ceramic layer thickness was modelled by a diffusion-based law, in agreement with several previous works [2,3,14-17, 31-36]. In fact, the coating growth is determined by the

reaction between carbon and CFE at the coating-liquid phase interface. Depending on the reaction controlling step, the coating thickness is proportional to the amount of C (N) or CFE available for the reaction. Nevertheless, for the bath conditions used here, CFE alternative controlling must be faster due to the high metallic atoms content and mobility in the liquid phase [10]. Therefore, one can reasonably assume that the reaction is controlled by carbon (N) diffusion and the layer thickness, y , is proportional to its diffusion distance:

$$y = A\sqrt{Dt} = A\sqrt{D_0 \exp(-Q/RT)t} \quad (1)$$

where D is the diffusion coefficient, D_0 the pre-exponential constant for diffusion, R the universal constant of perfect gases (8.31 J/mol K), Q the activation energy for carbon diffusion, t and T the treating time and temperature, respectively, and A is a constant depending on C (N) concentration in the substrate, the reaction stoichiometry and carbide (nitride)molar volume.

Equation 1 may be reduced to the well-known relation[2,3,14-17, 31-36]:

$$y = \sqrt{K_0 \exp(-Q/RT)t} \quad (2)$$

if $K_0 = D_0 A^2$.

The experimental evolution of thickness as a function of temperature and time is shown in Figures 10 and 11, respectively. The obtained diagrams clearly point out the very good agreement between theory and experimental findings.

On the basis of the obtained results, some considerations can be advanced:

- treatments in Cr12 bath produce thicker coatings than in FeV12 bath;
- when nitrided substrate is used, it accelerates the layer growth (if a layer is effectively produced);
- the effect of time and temperature can be modelled by diffusion law.

Equation (2) can be linearized by using the natural logarithm of the thickness:

$$\ln(y) = \frac{1}{2} (\ln(K_0 t) - Q/RT) \quad (3)$$

The experimental data can be therefore linearly fitted by using Eq (3) (Fig. 12) and this allows the determination of Q and K_0 .

The results are summarized in Table IV. For V_6C_5 coating growth, the results well compare to those previously published [2, 27]; conversely, for chromium carbide the activation energy is lower than that measured by Sen [16]. This difference can be related to the different substrate (AISI 4140\ AISI D2) and TRD techniques used (molten salts/pack method).

Similar activation energy values have been obtained for the other substrate/bath conditions.

One can observe that Q is always much larger than the activation energy for carbon diffusion in austenite (123 kJ/mol); this means that carbon diffusion in steel substrate is not the controlling step of the process. In addition, Q is more similar to the carbon self-diffusion energy barrier reported in literature for the produced carbides (244-280 kJ/mol for vanadium carbide and 167-188 kJ/mol for chromium carbide [30]). The difference between the measured data and the literature ones can be accounted for by the differences in carbide stoichiometry, substitutional impurities (i.e. the presence of limited amount of iron in the coatings as determined by EDS) and differences in the temperature range (825-1000°C in the present work, 1200-2600°C from the literature) [30]. Therefore, this work is supporting the thesis that the coating growth is controlled by carbon diffusion within the coating itself.

On the other hand, different K_0 parameters are obtained, this being related to different coating molar volume and reaction stoichiometry. In particular, K_0 is higher for Cr_7C_3 than for V_6C_5 coatings, as a result of a lower carbon/metal ratio. In other words, one chromium and one vanadium mole needs 0.43 and 0.83 moles of carbon, respectively, for completing the reaction. Being carbon diffusion the controlling step of the reaction, pre-exponential constant is higher for Cr_7C_3 than for V_6C_5 .

In addition, one can suggest that the K_0 parameter for VN coatings is higher than for V_6C_5 because of the higher amount of CFE/NFE in the nitrided substrate.

The thickness of the composite layers was, as expected, in between those measured for Cr12 and FeV12 baths. The measured activation energy for the mixed coatings lies in the range 197-200 kJ/mol, very close to those calculated for the single-phase layers. Conversely, the K_0 value increases with the chromium load in the bath as a result of the higher chromium carbide concentration in the coating. The estimated values for K_0 were 60, 67 and 72 mm²/s for Cr4FeV8, Cr6FeV6 and Cr8FeV4, respectively.

Vickers micro-hardness tests were performed on the cross section of the specimens treated at 1000°C in the different baths. Very interesting results were found on carbides-containing coatings: hardness values of 2451 ± 236 HV_{0.02} and 1825 ± 146 HV_{0.02} were measured on coatings produced on Q/T substrate treated in FeV12 and Cr12 bath, respectively. Biphasic coatings were characterized by intermediate values (Fig. 13) because of the presence of both carbides, V₆C₅ and Cr₇C₃. The hardness of such composite coatings does not follow exactly the rule of mixture, which is widely used for estimating the hardness of cermet [20-22], the measured values being larger than those theoretically estimated. This can be explained considering that Cr₇C₃ phase contains also some vanadium in solid solution, which is responsible for a hardening effect.

The hardness of VN coating was lower and was estimated to 1717 ± 170 HV_{0.02}. All the values measured are compatible with the literature data [23,24,29].

The surface finishing of the ceramic coatings was analysed by the profilometer on samples treated at 1000°C: the results are summarized in Table V. Although the coating process worsens the initial R_a value, roughness remains always below 0.5 µm for the hardened and tempered substrate and around 1 µm for the nitrided substrate.

The relatively higher roughness values of the VN coating is probably due to the presence of some salt particles adherent to the surface (which can not be easily removed) and with the non perfectly flat coating-substrate interface.

Also the biphasic layers are characterized by good surface finish; therefore, the two phase formation and the thermal stresses associated to the different thermal expansion coefficient do not influence the surface quality to a significant extent.

Finally, some considerations should be advanced about the nitrided samples treated in Cr12 bath. In this case no significant coatings were produced. Only some weak chromium nitrides (CrN and $(\text{Cr,Fe})_2\text{N}_{1-x}$) peaks were observed by XRD, their intensity becoming more intense by decreasing the treating temperature. On the other hand, it has to be reminded that previous works on TRD treatment [11-13] demonstrated the formation of a nitride-carbonitride layer on nitrided steel at low temperature (550-700°C).

The experimental results collected in the present work seem to indicate that the reaction is limited mainly by the thermodynamic of the system and not by the kinetic, which should be faster at higher temperature. A thermodynamic analysis of the process can be performed by using the Ellingham diagram for nitrides formation (Fig. 14). Such diagram, calculated from the thermochemical data published by Barin [26] and Knacke et al. [25], shows the relationship between temperature and free energy of formation of different nitrides (per moles of N_2). In the calculation it has been assumed that the free energy of $[\text{N}]$ is equal to one half the free energy of the N_2 gas phase.

According to Figure 14, one can observe that iron nitride (Fe_4N) is not thermodynamically stable; therefore, during the TRD treatment, it should undergo to thermal decomposition generating $\alpha\text{-Fe}$ and N . In addition, Figure 14 clearly shows that ΔG^0 for chromium nitride formation, especially at high temperature, is very high; in other words, the thermodynamic driving force of the reaction is weak. In fact, in standard conditions, ΔG^0 for the reaction producing Cr_2N phase (the most stable among the chromium nitrides) is negative, although included in the range between -21.5 / -16.0 kcal/mol, which are values much higher than the free energy for VN formation (between -58.8 and -52.1 kcal/mol) [25]. It should be pointed out that the working conditions during the process are really far from the standard condition:

therefore, it is not very surprising that chromium nitride does not form effectively and that it appears at low temperature (825°C) sporadically.

4 Conclusions

Hard carbide/nitride coatings can be obtained by Thermo-Reactive Diffusion and Deposition carried out in Cr/V containing – liquid borax baths on 42CrMoS4 steel. By using different processing conditions (bath composition, time, temperature, steel conditions – bare or nitride) coatings with different compositions and microstructure can be produced.

Chromium (Cr_7C_3 or $(\text{Cr,Fe})_7\text{C}_3$) and vanadium (V_6C_5) carbide coatings can be obtained in the temperature range of 825-1000°C. The ceramic coatings are characterized by a clean and flat coating-steel interface, excellent surface finish, good adhesion, absence of cracks and small amount or absence of pores. Furthermore, also biphasic layers can be produced.

Vanadium nitride (VN) coatings are produced on nitrated substrate in the same temperature range. The surface finish of the coatings is almost as good as in the carbides-containing coatings and the interface with the substrate is not perfectly flat. No chromium nitride coatings could be obtained by using the working conditions selected in the present work. The growth kinetic of the coatings can be modelled by a diffusive law. The thickness is related to the time by a parabolic relationship and to the temperature by an Arrhenius-like trend.

Carbide coatings are characterized by outstanding micro-hardness values, ranging from $2451 \pm 236 \text{ HV}_{0.02}$ for V_6C_5 to $1825 \pm 146 \text{ HV}_{0.02}$ for Cr_7C_3 .

References

- [1] R. F. Bunshah, Handbook of Hard Coatings: Deposition Technologies, Properties and Application, Noyes Publications, New Jersey, 2001.
- [2] X. Fan, Z. Yang, Y. Zhang, H. Che, Evaluation of vanadium carbide coatings on AISI H13 obtained by thermo-reactive deposition/diffusion technique, Surf. & Coat. Technology, 205 (2010) 641–646.
- [3] T. Arai, Thermoreactive Deposition/Diffusion Process for Surface Hardening of Steels, in: ASM Handbook, tenth ed., ASM International, 1991, Volume 4- Heat Treating.
- [4] S. Taktak, S. Ulu, Wear behaviour of TRD carbide coatings at elevated temperatures, Industrial Lubrication and Tribology, 62 (2010) 37-45.
- [5] S. Sen, Influence of chromium carbide coating on tribological performance of steel, Mater. and Design, 27 (2006) 85–91.
- [6] U. Sen, Friction and wear properties of thermo-reactive diffusion coatings against titanium nitride coated steels, Mater. and Design, 26 (2005) 167–174.
- [7] C. Oliveira, C. Benassi, L. Casteletti, Evalutation of hard coatings obtained on AISI D2 steel by thermo-reactive deposition treatmen, Surf. & Coat. Technology, 201 (2006) 1880-1885.
- [8] U. Sen, S. Sedar, S. Sen, Niobium boride coating on AISI M2 steel by boro-niobizing treatment, Mater. Letters, 62 (2008) 2444–2446.
- [9] M. Aghaie-Khafri, F. Fazlalipour, Vanadium carbide coatings on die steel deposited by the thermo-reactive diffusion technique, J. of Phys. and Chemistry of Solids, 69 (2008) 2465–2470
- [10] T. Arai, Development of carbide and nitride coatings by thermo-reactive deposition and diffusion, in: Proceedings of the Third International Conference on Surface Modification Techniques III, Neuchatel, Switzerland, 1989, pp. 587–598.
- [11] H. Cao, C. Wu, J. Liu, C. Luo, G. Zou, A novel duplex low-temperature chromizing process at 500°C, J. of Mater. Sci and Technology, 23 (2007) 823-827.
- [12] G. Khalaj, A. Nazari, S. M. M. Khoie. M.J. Khalaj, H. Pouraliakbar, Chromium carbonitride coating produced on DIN 1.2210 steel by thermo-reactive deposition technique: thermodynamics, kinetics and modeling, Surf. & Coat. Technology, 225 (2013) 1-10.
- [13] H. Cao, C.P. Luo, J. Liu, G. Zou, Phase transformations in low-temperature chromized 0.45 wt.% C plain carbon steel, Surf. & Coat. Technology, 201 (2007) 7970-7977.
- [14] M. Aghaie-Khafri, F.Fazlalipour, Kinetics of V(C,N) coating produced by a duplex surface treatment, Surf. & Coat. Technology, 202 (2008) 4107–4113.
- [15] U. Sen, Kinetics of niobium carbide coating produced on AISI 1040 steel by thermo-reactive deposition technique, Mater. Chemistry and Phys., 86 (2004) 189–194.
- [16] S. Sen, A study on kinetics of CrxC-coated high-chromium steelby thermo-reactive diffusion technique, Vacuum, 9 (2005) 63–70.

- [17] C. Wei, F. Chen, Thermoreactive depositio/diffusion coating of chromium carbide by contact free method, *Mater. Chemistry and Phys.*, 91 (2005) 192–199.
- [18] D. Fabijanic, G. Kelly, J. Long, P. Hodgson (2005), A nitrocarburising and low temperature chromising duplex surface treatment, *Mater. Forum*, 29 (2005) 77-82.
- [19] H. K. Bhadeshia, R. Honeycombe, *Steel: Microstructure and Properties*, third ed., Elsevier Ltd, Oxford, 2006.
- [20] R.W. Armstrong, The Hardness and Strength Properties of WC-Co Composites, *Mater.*, 4 (2011) 1287-1308.
- [21] Y.V. Milman, S. Luyckx, I. Nortrop, Influence of Temperature, grain size and cobalt content on the Hardness of WC-Co alloys, *International J. of Refractory Metals & Hard Mater.*, 7 (1999) 39-44.
- [22] R. Warren, *Ceramic Matrix Composites*, Blackie, Glasgow, 1991.
- [23] H. Pierson, *Handbook of Refractory Carbide and Nitride*, Noyes Publications, New Jersey, 1996.
- [24] M. Peterson, W. Winner, *Wear Controll Handbook*, The american Society of Mechanical Engineers, New York, 1980.
- [25] O. Knacke, O. Kubaschewski, K. Hesselman, *Thermochemical Properties of Inorganic Substances*, Springer, Berlin, 1991.
- [26] I. Barin, *Thermochemical Data of Pure Substances*, third ed., VCH, Weinheim, 1995.
- [27] X.S. Fan, Z.G. Yang, C. Zhang, Y.D. Zhang, Thermo-reactive deposition processed vanadium carbide coating: growth kinetics model and diffusion mechanism, *Surf. & Coat. Technology*, 208 (2012) 80–86.
- [28] F.E. Castillejo, J.J. Olaya, J.M. Arroyo-Osorio, Nb–Cr complex carbide coatings on AISI D2 steel produced by the TRD process, *J. Braz. Soc. Mech. Sci. Eng.*, 37 (2015) 87-92.
- [29] U. Sen, M. Uzun, S. Sen, Tribological Properties of Vanadium Nitride Coated AISI 52100 Steel, *Advanced Materials Research*, 445 (2012) 643-648.
- [30] H.J. Matzke, V.V. Rondinella, Diffusion in carbides, nitrides, hydrides and borides, in: D.L. Beke (Ed.), *Diffusion in Semiconductors and Non-Metallic Solids*, Springer, Berlin, 1999.
- [31] M. Aghaie-Khafri , F. Fazlalipour, Vanadium carbide coatings on die steel deposited by the thermo-reactive diffusion technique, *J. Physics and Chemistry of Solids*, 69 (2008) 2465–2470.
- [32] U. Sen, Kinetics of titanium nitride coatings deposited by thermo-reactive deposition technique, *Vacuum* 75 (2004) 339–345.
- [33] X.S. Fan, Z.G. Yang, C. Zhang, Y.D. Zhang, Thermo-reactive deposition processed vanadium carbide coating: growth kinetics model and diffusion mechanism, *Surf. & Coat. Technology*, 208 (2012) 80–86.
- [34] G. Khalaj, A. Nazari, S. M. Mousavi Khoie, M. Javad Khala, H. Pouraliakbar, Chromium carbonitride coating produced on DIN 1.2210 steel by thermo-reactive deposition

technique: Thermodynamics, kinetics and modeling, Surf. & Coat. Technology, 225 (2013) 1–10.

[35] X. Liu, H. Wang, D. Li, Y. Wu, Study on kinetics of carbide coating growth by thermal diffusion process, Surf. & Coat. Technology, 201 (2006) 2414–2418.

[36] F. S. Chen, P. Y. Lee, M. C. Yeh, Thermal reactive deposition coating of chromium carbide on die steel in a fluidized bed furnace, Mater. Chemistry and Physics 53 (1998) 19–27.

	C	Mn	S	Cr	Mo	Si
Nominal	0.38/0.45%	0.6/0.9%	0.02/0.04%	0.9/1.2	0.15/0.30%	0.4% max
Actual	0.4%	0.8%	0.3%	0.9%	0.2%	0.2%

Table I: Chemical composition of the substrate.

	Used bath				
	Cr12	Cr8FeV4	Cr6FeV6	Cr4FeV8	FeV12
Borax	85	85	85	85	85
Chromium	12	8	6	4	0
Ferrovandium	0	4	6	8	12
Aluminium	3	3	3	3	3

Table II: Labelling and composition (wt%) of the used baths.

Used bath	Cr12	Cr8FeV4	Cr6FeV6	Cr4FeV8	FeV12
Substrate	Q/T - N	Q/T	Q/T	Q/T	Q/T - N
T1= 825°C	4 h	4 h	4 h	4 h	4 h
T2= 900°C	2 h /4 h /16 h	4 h	4 h	4 h	2 h /4 h /16 h
T3=1000°C	4 h	4 h	4 h	4 h	4 h

Table III: Different combinations of the main process parameters: time, temperature, substrate and bath.

Q/T (Cr12)		Q/T (FeV12)		N (FeV12)	
Q (kJ/mol)	K ₀ (mm ² /s)	Q (kJ/mol)	K ₀ (mm ² /s)	Q (kJ/mol)	K ₀ (mm ² /s)
205	102	204	51	203	63

Table IV: Activation energy and K₀ values for the different treatments.

	Q/T					N
	Cr12	Cr8FeV4	Cr6FeV6	Cr4FeV8	FeV12	FeV12
R _a (μm)	0.25	0.20	0.30	0.40	0.35	1.2

Table V: Surface roughness measured on the different coatings.

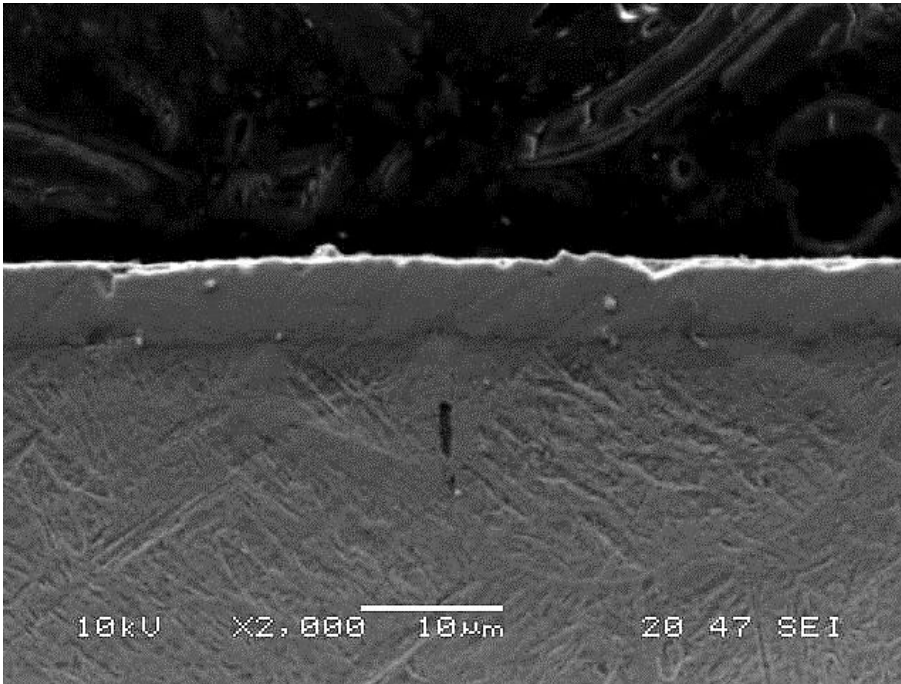


Figure 1: Chromium carbide layer produced at 900°C (16 h treatment) on Q/T steel in Cr12 bath.

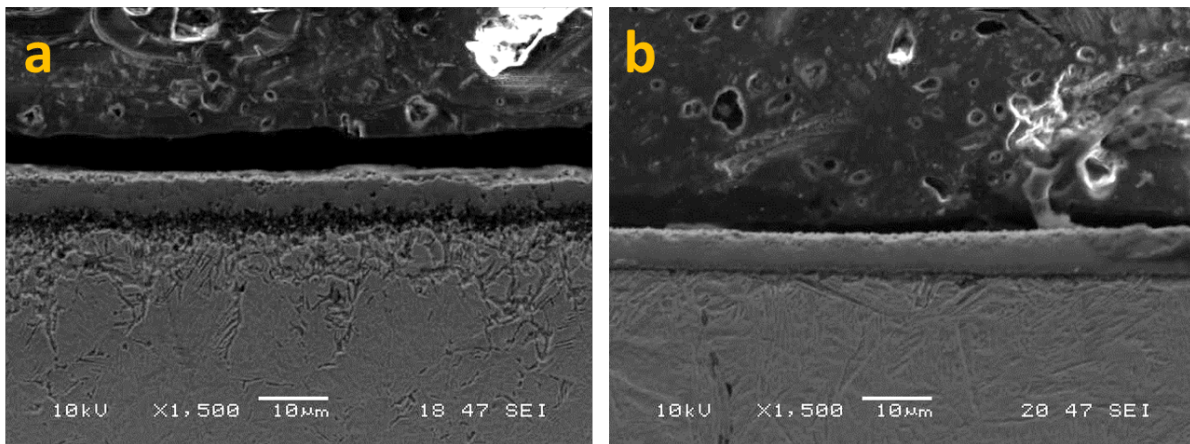


Figure 2: Ceramic layers layer produced at 900°C for 16 h on N (a) and Q/T (b) substrate in FeV12 bath.

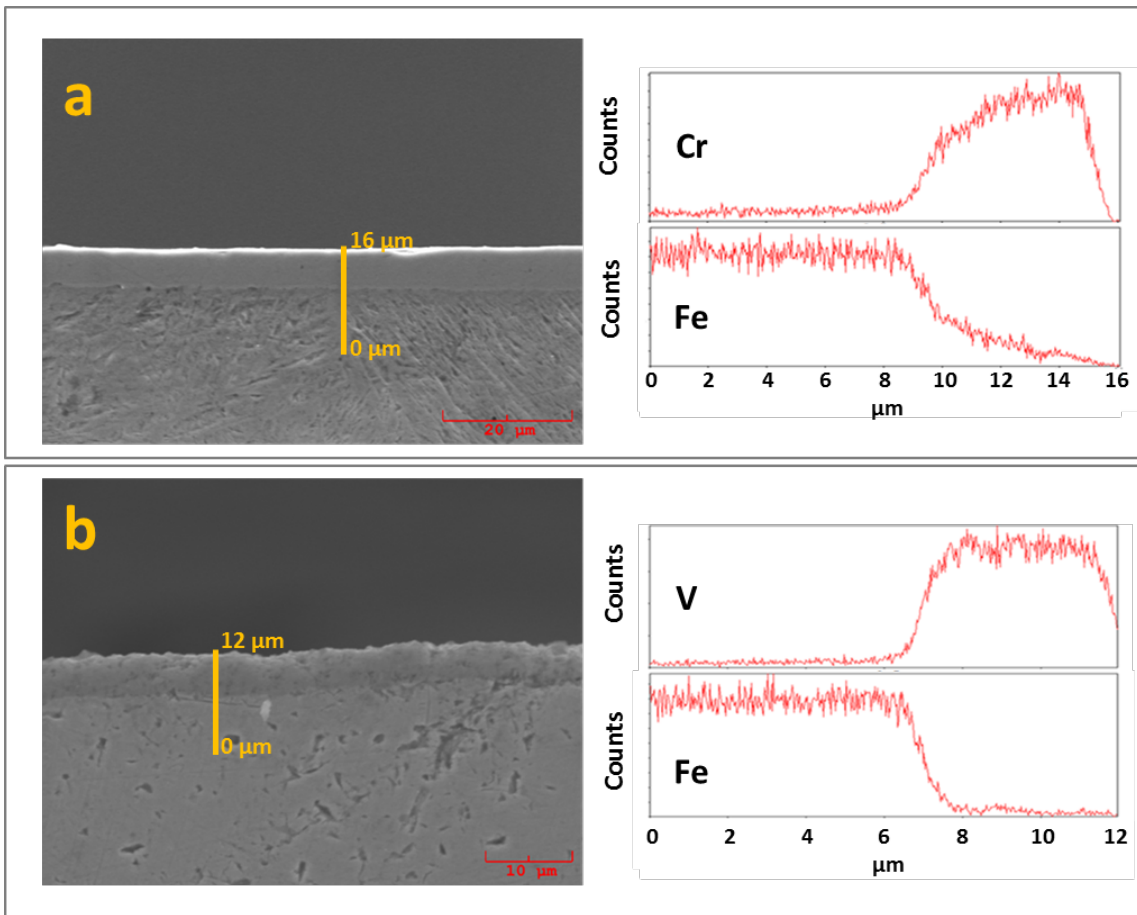


Figure 3: EDS linescan obtained on polished cross section of a chromium (Cr12 bath, 900°C, 16 h) (a) and vanadium (FeV12 bath, 900°C, 16 h) (b) carbide coatings. The linescan path is shown on the micrographs.

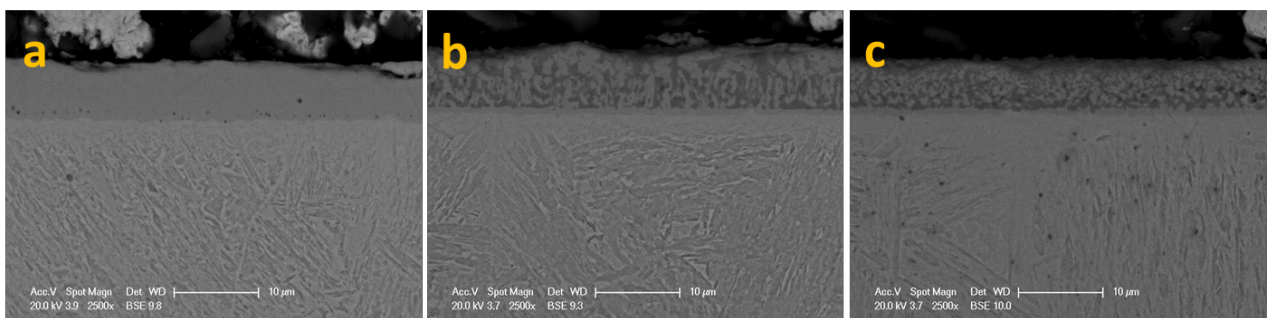


Figure 4: SEM micrographs of samples treated at 1000°C for 4 h in Cr₈FeV₄ (a), Cr₆FeV₆ (b) and Cr₄FeV₈ (c) baths.

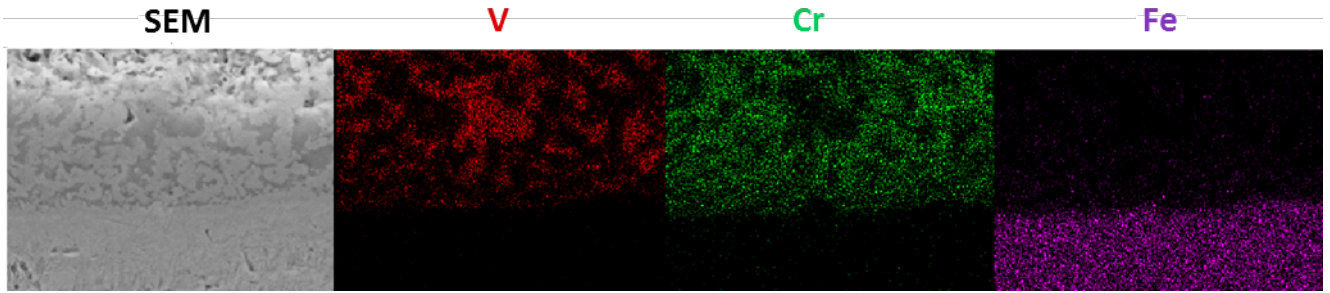


Figure 5: Biphasic coating obtained with Cr6FeV6 bath at 1000°C. The distribution map of V, Cr and Fe is shown underneath. .

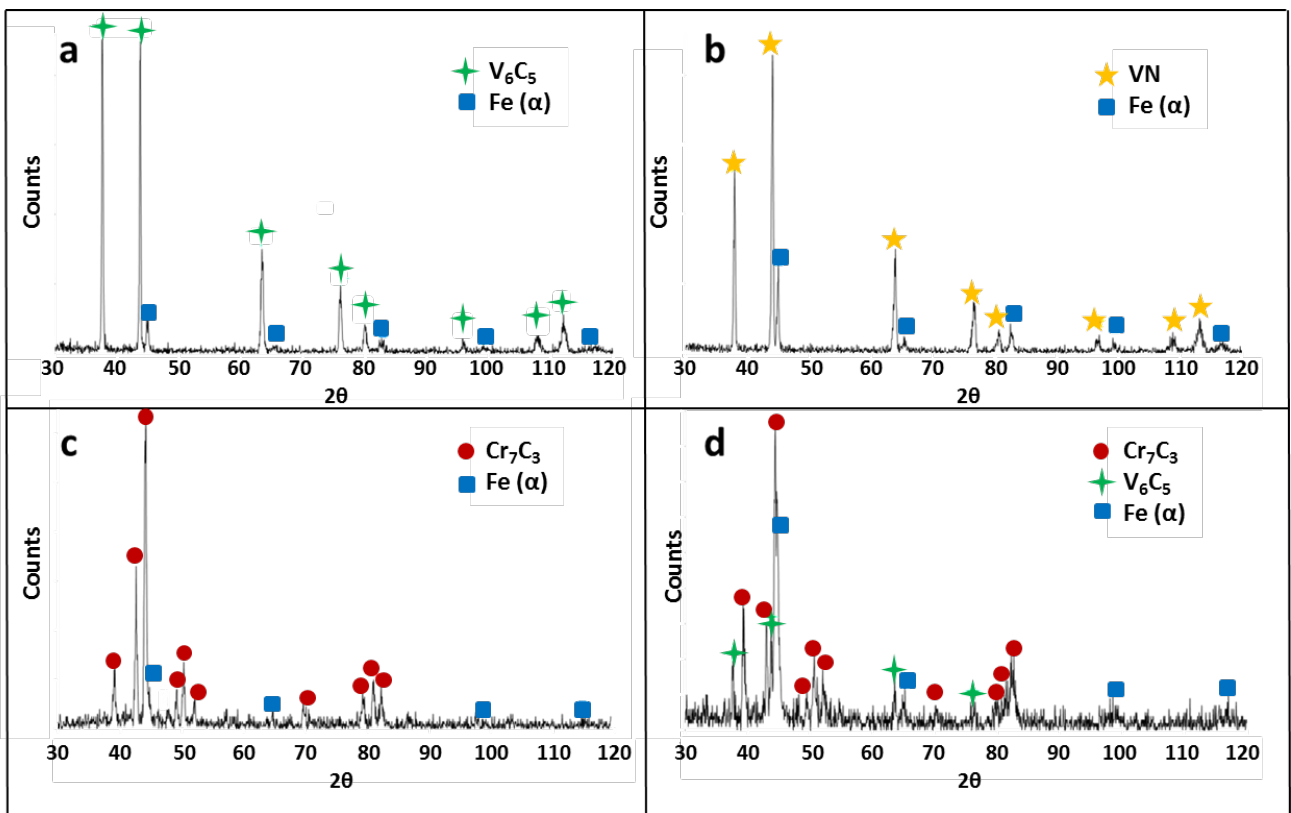


Figure 6: XRD spectra collected on coatings produced at 1000°C for 4 h: Q/T in FeV12 bath (a), N in FeV12 bath (b), Q/T in Cr12 bath (c) and Q/T in Cr6FeV6 bath (d).

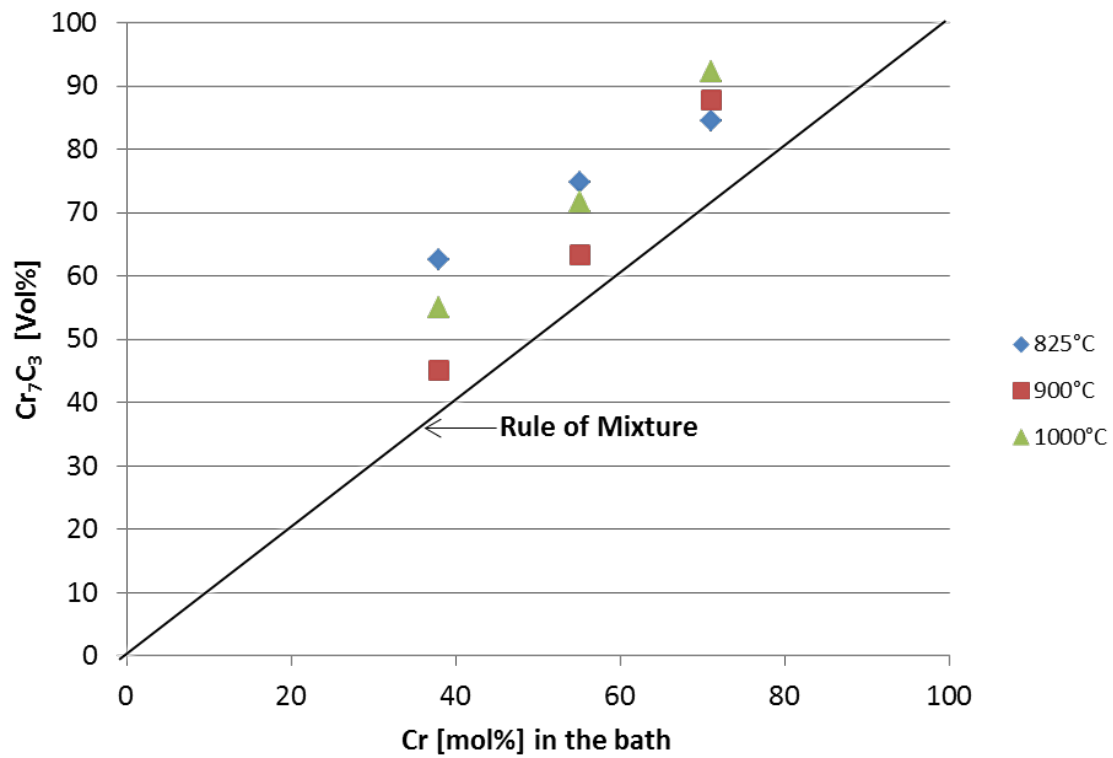


Figure 7: Mineralogical composition of the coatings as a function of molar CFE composition in the bath. A clear deviation from the role of mixture is present.

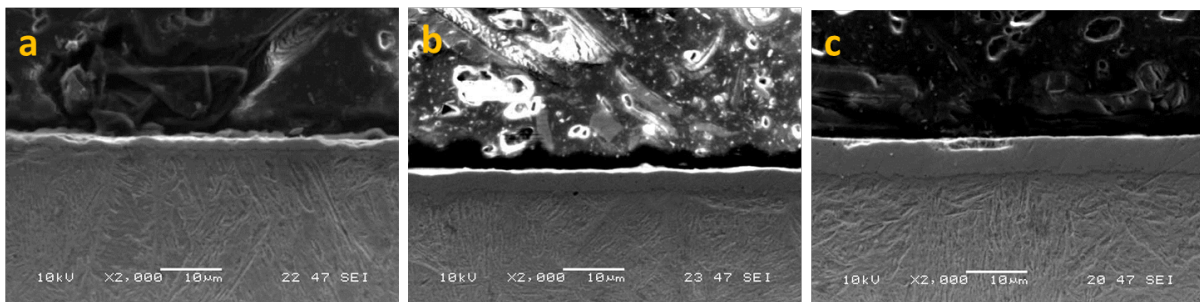


Figure 8: Chromium carbide coating evolution as a function of treating time at 900°C: (a) 2 h, (b) 4 h and (c) 16 h.

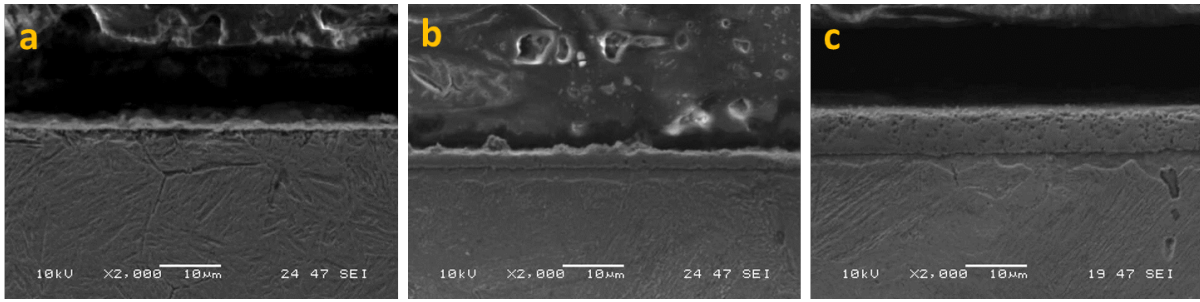


Figure 9: Vanadium carbide coatings produced with 4 h treatments at different temperatures. On the left (a) a ceramic layer obtained at 825°C, in the centre (b) at 900°C and on the right (c) at 1000°C.

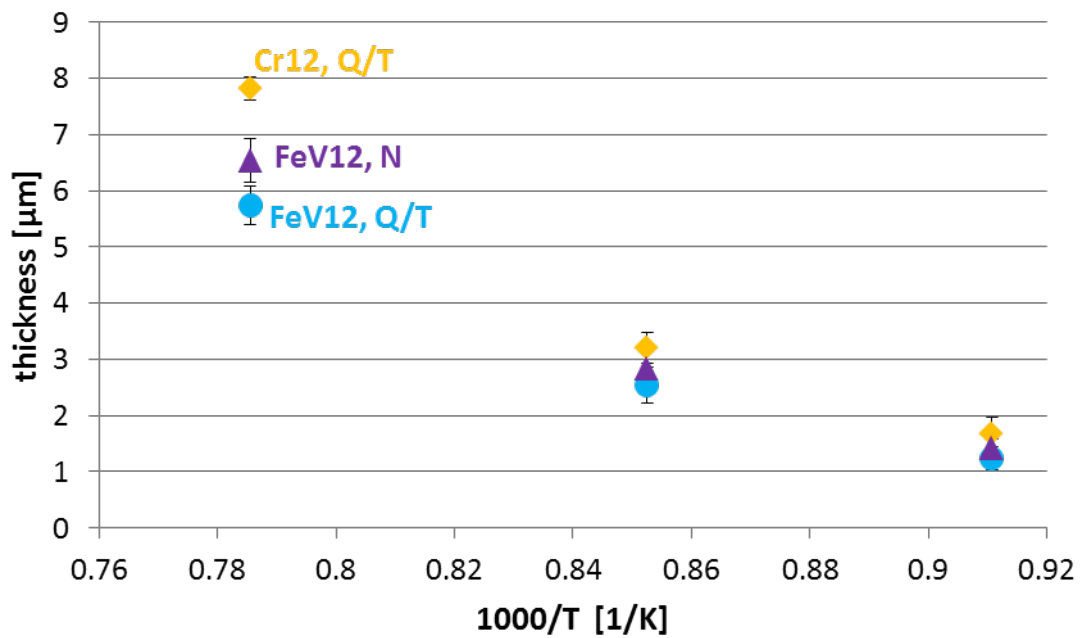


Figure 10: Coating thickness, obtained with 4 h treatments, as a function of $1000/T$.

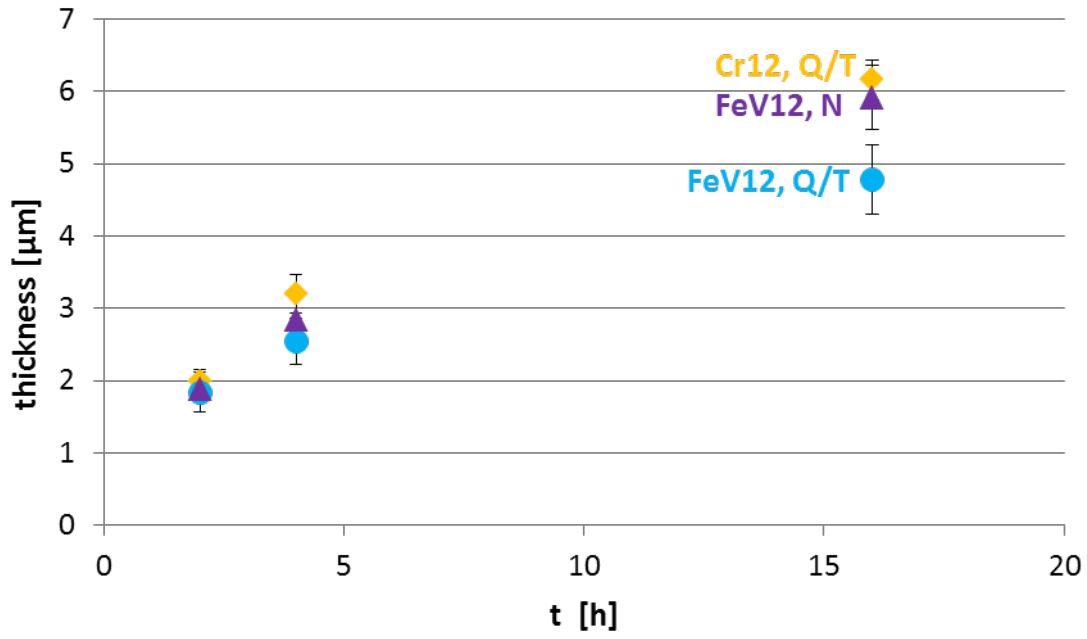


Figure 11: Coating thickness obtained at 900°C at different treating time.

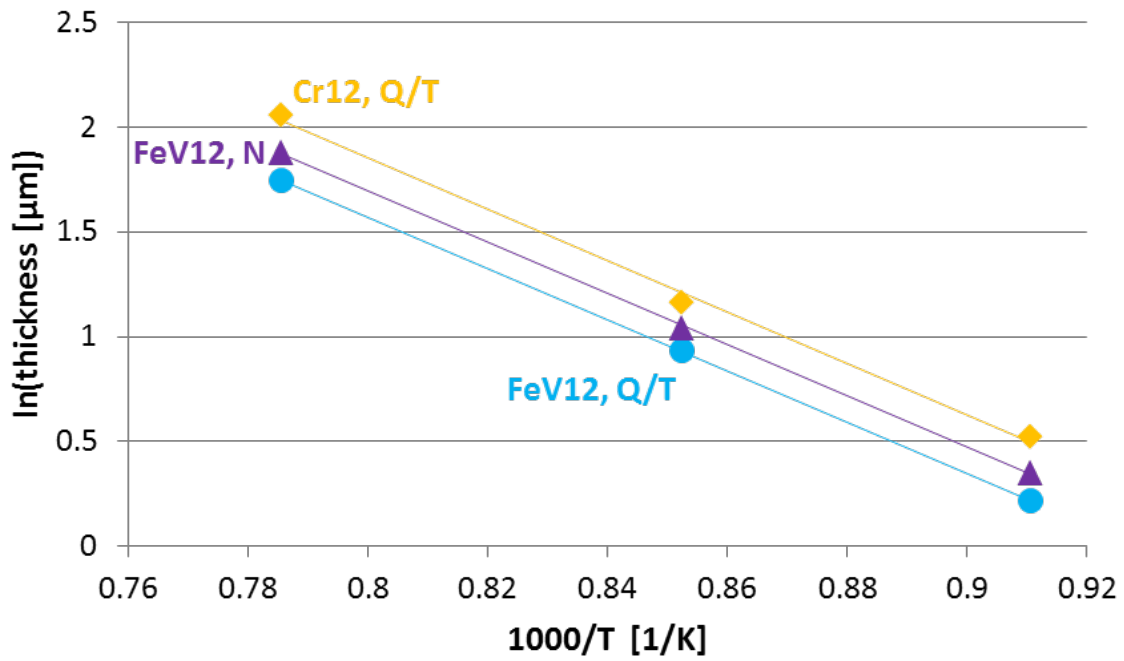


Figure 12: Thickness as a function of $1000/T$. Continuous lines represent the fitting curve determined on the basis of Eq. (2).

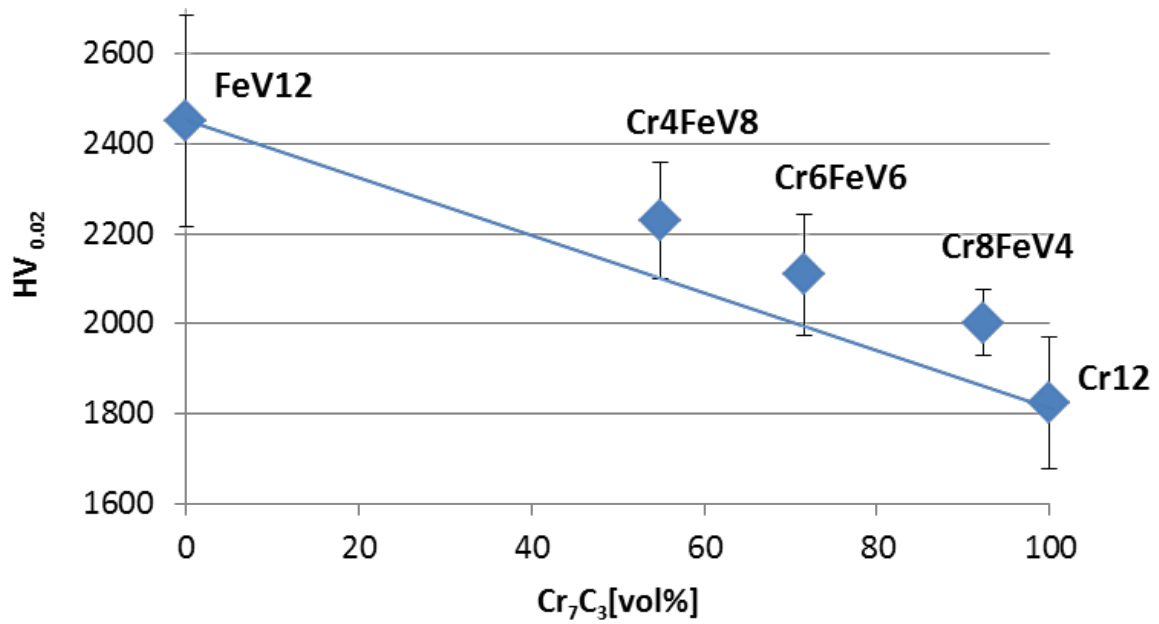


Figure 13: Hardness of the coatings produced in the different baths as a function of Cr_7C_3 phase content. The continuous line represents the role of mixture estimate.

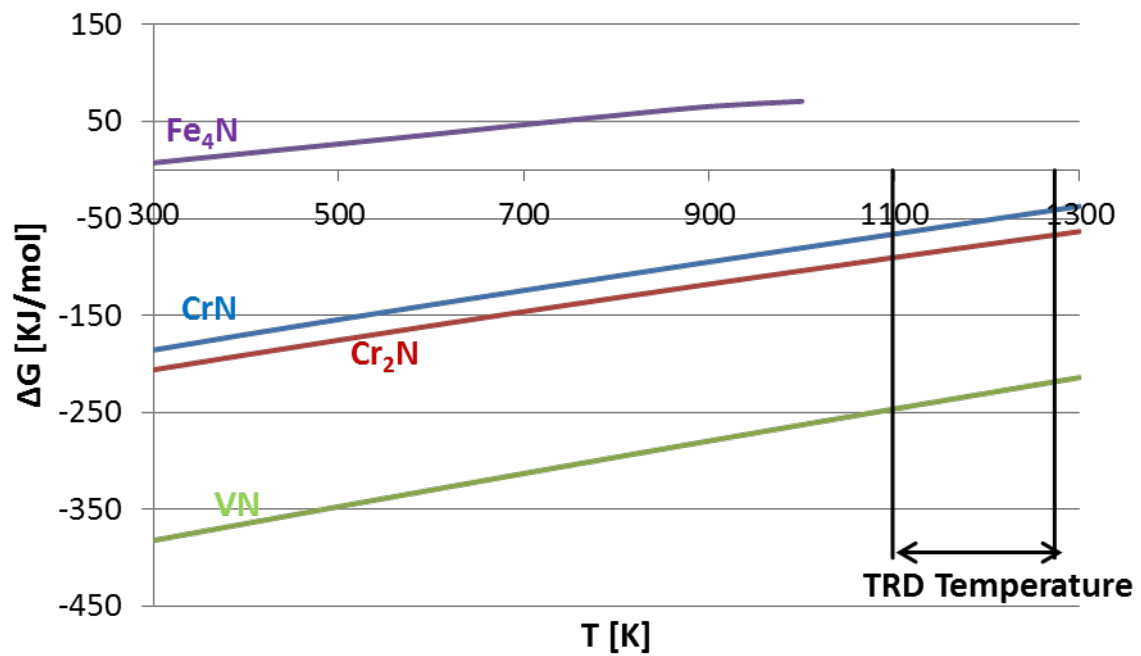


Figure 14: Ellingham diagram for nitrides formation.